SYSTEMATIC REVIEW

The utilization of positron emission tomography in the evaluation of renal health and disease

Kwame Anokye Amoabeng[1] · Sanna Laurila[2,3] · Luis Eduardo Juárez-Orozco[4,5] ·
Anne Beate Langeland Marthinsen[1,6] · Dariusz Moczulski[7] · Eleni Rebelos[8] · Prince Dadson[8,9]

Abstract

Purpose Positron emission tomography (PET) is a nuclear imaging technique that uses radiotracers to visualize metabolic processes of interest across different organs, to diagnose and manage diseases, and monitor therapeutic response. This systematic review aimed to characterize the value of PET for the assessment of renal metabolism and function in subjects with non-oncological metabolic disorders.

Methods This review was conducted and reported in accordance with the PRISMA statement. Research articles reporting "kidney" or "renal" metabolism evaluated with PET imaging between 1980 and 2021 were systematically searched in Medline/PubMed, Science Direct, and the Cochrane Library. Search results were exported and stored in RefWorks, the duplicates were removed, and eligible studies were identified, evaluated, and summarized.

Results Thirty reports met the inclusion criteria. The majority of the studies were prospective (73.33%, $n = 22$) in nature. The most utilized PET radiotracers were ^{15}O-labeled radio water ($H_2{}^{15}O$, $n = 14$) and ^{18}F-fluorodeoxyglucose (^{18}F-FDG, $n = 8$). Other radiotracers used in at least one study were 14(R,S)-(18)F-fluoro-6-thia-heptadecanoic acid (^{18}F-FTHA), ^{18}F-Sodium Fluoride (^{18}F-NaF), ^{11}C-acetate, 68-Gallium (^{68}Ga), ^{13}N-ammonia (^{13}N-NH$_3$), Rubidium-82 (^{82}Rb), radiolabeled cationic ferritin (RadioCF), ^{11}C-para-aminobenzoic acid (^{11}C-PABA), Gallium-68 pentixafor (^{68}Ga-Pentixafor), 2-deoxy-2-F-fluoro-D-sorbitol (F-FDS) and ^{55}Co-ethylene diamine tetra acetic acid (^{55}Co-EDTA).

Conclusion PET imaging provides an effective modality for evaluating a range of metabolic functions including glucose and fatty acid uptake, oxygen consumption and renal perfusion. Multiple positron emitting radiolabeled racers can be used for renal imaging in clinical settings. PET imaging thus holds the potential to improve the diagnosis of renal disorders, and to monitor disease progression and treatment response.

Keywords Renal systems · Metabolic disease · Metabolism · Positron emission tomography

---

Kwame Anokye Amoabeng and Sanna Laurila contributed equally to this work.

✉ Prince Dadson
pryada@utu.fi

1 Department of Physics, Norwegian University of Science and Technology, Trondheim, Norway

2 Turku PET Centre, Turku University Hospital, Turku, Finland

3 Heart Center, Turku University Hospital, Turku, Finland

4 Department of Cardiology, Heart and Lung Division, University Medical Centre Utrecht, Utrecht, The Netherlands

5 Department of Cardiology, University of Groningen, University Medical Center Groningen, Groningen, The Netherlands

6 Department of Radiotherapy, Cancer Clinic, St. Olav's University Hospital, Trondheim, Norway

7 Department of Internal Medicine and Nephrodiabetology, Medical University of Łódź, Łódź, Poland

8 Turku PET Centre, University of Turku, Turku, Finland

9 Department of Clinical Medicine, University of Turku, Turku, Finland

🖄 Springer

Introduction

The kidneys are complex metabolic organs that perform osmoregulatory and key endocrine functions [1]. They effectively filter, remove, and reabsorb both essential and non-essential solutes from plasma, while contributing to the regulation of the acid–base balance in the body [2, 3]. They also play important roles in the metabolism of carbohydrates, proteins, and other nutrients [4]. Given their functional and metabolic roles, diseases affecting kidneys such as acute or chronic renal failure usually result in complex deleterious alterations in the overall physiological and metabolic processes in the body [5].

The kidneys utilize several different substrates such as lactate, free fatty acids, glutamine, 3-hydroxybutyrate, glycerol and citrate for the functional activities [6]. The preferred substrates for cellular respiration in the renal cortex include both short- and long-chain fatty acids and some amino acids [7]. In the outer medulla, lactate appears to be the preferred substrate over glucose [7]. And in the inner medulla, oxygen consumption is much lower than in the cortex, while glucose is the preferred metabolic substrate [6].

During the postabsorptive period, the kidneys account for 10% of the whole-body glucose utilization. Normally, approximately 180 g of glucose are filtered every 24 h and almost all of it are reabsorbed by means of the sodium/glucose cotransporter 2 (SGLT2) system, which is expressed in the early proximal tubules of the nephron [2, 3]. Most of the remaining glucose absorption is by sodium/glucose cotransporter 1(SGLT1) located at a more distal sections of the proximal tubules [8]. Importantly, the reabsorption of sodium ions is mainly due to the extremely high oxidative metabolism of the renal system [9].

Metabolic disease/disorder is characterized by the disruption in normal metabolism which affects the performance of critical biochemical reactions involving the processing or transport of proteins (amino acids), carbohydrates (glucose), and lipids (fatty acids) [10]. Moreover, metabolic disease is associated with oxidative stress and mitochondrial dysfunction [10]. Previous studies have reported that individuals with metabolic abnormalities are at an increased risk of renal dysfunction, including chronic kidney disease which may lead to kidney failure and end-stage renal disease [11–14].

Positron emission tomography (PET) is a nuclear medicine-based imaging technique that can functionally evaluate metabolic processes within the body by the use of non-nephrotoxic tracer compounds [15, 16]. Its application has been extensive in the study of a variety of organs, and it is currently considered the gold standard for measuring tissue metabolic rates in vivo. PET data can be analyzed either semiquantitatively (through standardized uptake rate-SUV) or quantitatively (through graphical analysis, fractional uptake rate, compartmental models). The latter requiring determination of plasma input function, thus tracking the tracer uptake in the tissue of interest in respect to its availability in the circulation [17].

While PET applications in studies of brain [18], heart [19], liver [20], skeletal muscle [21] and adipose tissue [22, 23] are well established, there have been challenges in its implementation for the study of the kidneys. We believe, however, that renal PET has begun to demonstrate its unique potential in providing useful information in a relatively non-invasive manner. The present systematic review, therefore, aimed to identify and summarize all available studies that have evaluated kidney physiology (i.e., renal perfusion, glomerular filtration rate, glucose, and fatty acid metabolism) and pathophysiology (i.e., renal failure, acute rejection following kidney transplantation, renal cysts) though PET imaging in non-oncological patients with metabolic disorders.

Methods

Eligibility criteria

Peer reviewed publications reporting on the utilization of PET imaging for the evaluation of renal (patho) physiology in humans (namely renal perfusion, glucose, and fatty acid metabolism) from 1980 to 2021 (based on the time span of the technique's existence) were included in this review. Editorials, letters, commentaries, perspectives, and conference abstracts were excluded together with PET studies involving oncological diseases with renal involvement. Only articles written in the English language were considered.

Information sources and search strategy

1. Words that relate to the system: renal, kidney, nephrology.
2. Words that relate to the technique: positron emission tomography.
3. Words that relate to the studied function: renal metabolism in metabolic disorders.

We searched the MEDLINE (through PubMed), Science Direct and Cochrane databases. These databases were selected, because they provide extensive international journals and are regularly updated with relevant resources covering medicine, health sciences and related topics. Reference lists of relevant articles were hand-searched to identify additional articles. Relevant articles were then exported to and managed in the RefWorks Citation Manager®.

Study selection

After the deletion of duplicates, all titles and abstracts were duly reviewed and screened against the eligibility criteria. All ineligible articles were removed. Full texts of all relevant articles were then retrieved.

Data items and collection process

This systematic review was conducted and reported in accordance with the Preferred Reporting Items for Systematic Review and Meta-Analyses (PRISMA) statement [24]. Data were extracted into a standardized data collection form. Extracted data included: first author, publication year, demographics, study design, limitations, major findings, conclusion, and remarks. Each study was read and reread to identify core methodological aspects, perform data reduction and when possible, some comparisons. Two reviewers independently abstracted the contents of each included study. The risk of bias was appraised using Joanna Briggs Institute Critical Appraisal Checklist for Qualitative Research [25]. Discrepancies and disagreements were resolved through a third independent researcher.

Results

A total of 2502 articles were identified. After removal of duplicates and screening based on titles and abstracts, 73 articles underwent a full-text review out of which thirty met the inclusion criteria (Fig. 1, Table 1). Designs included prospective (73.33%, $n = 22$), retrospective (16.12%, $n = 5$), cross-sectional (6.45%, $n = 2$), and observational studies (3.22%, $n = 1$) studies. Most of the studies used ^{15}O-labeled water ($n = 14$) or ^{18}F-fluorodeoxyglucose (^{18}F-FDG, $n = 8$) as the PET radiotracer. Tracers that were use in at least on study included ^{15}O, ^{11}C-acetate ^{18}FFTHA, RadioCF, ^{82}Rb, ^{11}C-PABA, F-NaF, ^{18}F-FDS, ^{68}Ga-pentixafor, ^{82}Rb, ^{13}N-ammonia, and ^{68}Ga-EDTA (Table 1).

Renal perfusion

A radiopharmaceutical is suitable for renal perfusion quantification if it shows high perfusion-rate-independent extraction from arterial blood in its first-pass transit through the renal capillaries [26]. The most commonly used PET tracer for perfusion measurement has been oxygen-15 radiolabeled water (H_2^{15}O, radiowater) $n = 15$ [16, 27–40]. One study also reported that carbon-15 labeled acetate (^{11}C-acetate) can be used for the same purpose [37]. A one-compartment model was used for the quantification of these tracers. Other tracers, which are not entirely freely diffusible, have also been used for perfusion quantification through implementation
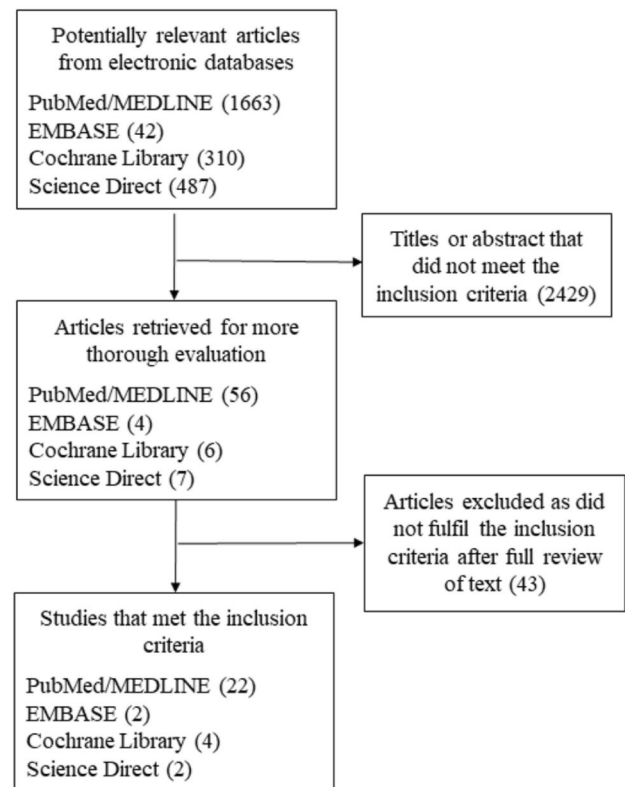

Potentially relevant articles from electronic databases
PubMed/MEDLINE (1663)
EMBASE (42)
Cochrane Library (310)
Science Direct (487)

Titles or abstract that did not meet the inclusion criteria (2429)

Articles retrieved for more thorough evaluation
PubMed/MEDLINE (56)
EMBASE (4)
Cochrane Library (6)
Science Direct (7)

Articles excluded as did not fulfil the inclusion criteria after full review of text (43)

Studies that met the inclusion criteria
PubMed/MEDLINE (22)
EMBASE (2)
Cochrane Library (4)
Science Direct (2)

Fig. 1 Study flow chart

of the two-compartment Patlak model namely, Nitrogen-13 labeled ammonia (^{13}N-ammonia) $n = 1$ [28] and rubidium-82 chloride (^{82}Rb) $n = 2$ (which behaves like a K^+ analogue and is very commonly used to measure myocardial perfusion) [41, 42].

Energy substrate metabolism

In a recent study that aimed to automatically quantify tracer uptake during euglycemic hyperinsulinemic clamp conditions, volume estimation by ^{18}FDG was comparatively inaccurate in the kidneys [43]. This was largely due to spillover from urine. Furthermore, 14(R, S)-[18F] fluoro-6-thia-heptadecanoate (^{18}F-FTHA) has been used to estimate cortical and medullar fatty acid uptake ($n = 1$) [38], while oxygen consumption has been quantified with ^{11}C-acetate $n = 1$ [37].

Inflammation

^{18}FDG has been shown to be useful in the noninvasive diagnostic workup in suspected allograft rejection $n = 2$ [44, 45]. In a small proof-of-concept study that included only two human subjects, Werner et al. suggested 2-deoxy-2-[18F] fluorosorbitol (^{18}F-FDS) as an alternative to ^{18}F-FDG in pediatric patients due to a lower radiation exposure

Table 1 Description of the utilization of positron emission tomography in renal system

Study, year	N	Tracer	Study design	Conclusion/major findings
Qiao et al., 2008	10	^{18}F-FDG	Retrospective	Excretive process of FDG could be simulated and the accumulation of FDG in urine and the plasma could be estimated
Laurent et al., 2000	6	^{15}O-water	Retrospective	PET using [15]O is a valuable method for measuring renal blood flow Limitation: Cost of procedure and the lack of availability of PET facilities
Normand et al., 2019	10	^{15}O-water, ^{11}C-acetate	Retrospective	Direct estimates of renal oxygen consumption as well as tissue perfusion can be obtained by PET with a single tracer [^{11}C] acetate
Inaba et al., 1989	8	^{15}O-water	Prospective	Renal plasma flow in the human kidney was determined by ^{15}O-water PET using a one-compartment model
Rebelos et al., 2019	38	[18]FFTHA, ^{15}O-water	Cross-sectional and intervention study	Morbidly obese subjects have increased renal FFA uptake and enhanced renal perfusion and months following bariatric surgery, renal perfusion is decreased, whereas renal FFA uptake remains high
Baldelomar et al., 2021	1	RadioCF	Prospective	Nephron mass could be mapped with the tracer in a donated human kidney
Keramida et al., 2020	74	[82]Rb	Retrospective	Kidney perfusion increased with regadenoson compared to baseline
Pajenda et al., 2020	37	^{18}F-FDG	Cross-sectional	Parameters obtained from FDG PET/MRI showed a possible predictive feature for renal recovery in solid organ kidney transplantation patients undergoing acute kidney injury
Guglielmo et al., 2020	12	^{18}F-FDG	Prospective	Automated quantification of tissue morphology and tracer uptake was conducted with FDG PET/MRI during insulin-glucose clamp conditions. Out of the measured organs, volume estimation was least accurate in the kidneys
Ruiz-Bedoya et al., 2020	3	^{11}C-PABA	Prospective	^{11}C-PABA was safe in humans and might be used as a radiotracer for functional renal imaging, providing high-quality spatiotemporal images with low radiation exposure
Jadoul et al., 2020	95	^{18}F-FDG	Prospective	The repeatability and reproducibility of the quantification of kidney allograft 18F-FDG uptake are both consistent, making it usable for disproving acute kidney allograft rejection
Oliveira-Santos et al., 2020	25	F-NaF	Retrospective	In a prospectively scanned high CV risk group without manifest CV disease, higher renal artery wall F-NaF activity is associated with superior predicted CV risk and lower GFR
Päivärinta et al., 2019	29	^{15}O-water	Prospective	Kidney transplant patients with stage 2–3 chronic kidney disease had higher renal vascular resistance than healthy controls, but kidney perfusion values did not differ between the groups. Perfusion correlated with doppler based resistance index in transplants
Werner et al., 2019	2	^{18}F-FDS	Prospective	^{18}F-FDS could be considered as an alternative to ^{18}F-FDG, due to its significantly smaller radiation exposure
Derlin et al., 2017	13	^{68}Ga-pentixafor	Prospective	^{68}Ga-pentixafor PET/MRI may enable the noninvasive detection of leukocytes in renal allografts
Lovinfosse et al., 2016	31	^{18}F-FDG	Prospective	^{18}F-FDG PET/CT may help noninvasively prevent avoidable kidney transplant biopsies with suspected allograft rejection
Tahari et al., 2013	8	[82]Rb	Prospective	Quantitative human kidney imaging with [82]Rb PET is feasible
Koivuviita et al., 2012	17	^{15}O-water	Observational	Angiographic severity of renal artery stenosis does not determine the perfusion response to revascularization
Damkjær et al., 2012	7	^{15}O-water	Prospective	Changes in renal perfusion are not necessarily involved in the natriuretic response to modest saline loading
Damkjær et al., 2010	9	^{15}O-water	Prospective	Medullar blood flow could be assessed, when PET/CT scans were conducted at baseline, during nitric oxide infusion and a nitric oxide synthase inhibitor infusion
Kudomi et al., 2009	6	^{15}O-water	Prospective	Measuring renal blood flow with ^{15}O-water is feasible
Minamimoto et al., 2006	40	^{18}F-FDG	Prospective	The Mean SUV of the left kidney was higher in healthy volunteers than patients suspected with renal failure

Table 1 (continued)

Study, year	N	Tracer	Study design	Conclusion/major findings
Juillard et al., 2002	8	^{15}O-water	Prospective	Renal blood flow increased rapidly after quinaprilat injection in patients with moderate chronic renal failure and hypertension
Middlekauff et al., 2000	77	^{15}O-water	Prospective	During sustained handgrip exercise, both the magnitude and duration of reflex renal vasoconstriction (measured by perfusion) are exaggerated in heart failure patients compared with normal healthy controls
Middlekauff et al., 1997	29	^{15}O-water	Prospective	A decrease in renal blood flow was observed in healthy subjects in response to static exercise
Middlekauff et al., 1995	18	^{15}O-water	Prospective	In patients with heart failure, there is an abnormality in cardiopulmonary baroreflex control of the forearm circulation but not the renal circulation
Nitzsche et al., 1993	20	^{13}N-ammonia ^{15}O-water	Prospective	Patlak graphical analysis with ^{13}N-ammonia renders accurate and reproducible estimates of renal cortical blood flow
Yamashita et al., 1988	6	^{68}Ga-EDTA	Prospective	Glomerular filtration rate could be measured with the tracer
Rasul et al., 2020	44	^{18}F-FDG	Prospective	Mean transit time of FDG decreased with 2 weeks of SGLT2i medication in T2D patients, shifting towards values of healthy controls
Geist et al., 2018	24	^{18}F-FDG	Prospective	GFR and ERPF can be assessed with dynamic FDG PET/MRI scans in healthy kidneys

PET tracers for the assessment kidney metabolism in humans; N, sample size; 15O-labeled radio water ($H_2^{15}O$), followed by ^{18}F-fluorodeoxyglucose (^{18}F-FDG);14(R,S)-(18)F-fluoro-6-thia-heptadecanoic acid (^{18}F-FTHA); ^{18}F-Sodium Fluoride (^{18}F-NaF); ^{11}C-acetate; 68-Gallium (^{68}Ga); 13N-ammonia (^{13}N–NH$_3$); Rubidium-82 (^{82}Rb); radiolabeled cationic ferritin (RadioCF); Carboxy-11C]4-Aminobenzoic acid (^{11}C-PABA); Gallium-68 pentixafor ([^{68}Ga]Ga-Pentixafor); 2-deoxy-2-F-fluoro-D-sorbitol (F-FDS); 55Co-ethylene diamine tetraacetic acid (^{55}Co-EDTA)

[46]. In one study, gallium labelled ^{68}Ga-pentixafor has been proposed as useful for detecting leukocytes in allografts when PET is combined with magnetic resonance imaging (MRI) [47].

Kidney function

In a study by Geist et al. [48], both the cortex and total kidney ^{18}FDG glomerular filtration rate obtained from regression analysis of Patlak plots were shown to have strong positive correlations with the reference value for estimated glomerular filtration rate (eGFR) [48]. $N = 2$ studies have quantified renal clearance rate of ^{18}FDG [49, 50]. One study calculated kidney function parameters from ^{18}FDG standardized uptake values and time activity curves [51]. Parallelly, Minamimoto et al. [52] showed that mean ^{18}FDG SUV in the kidney is higher in healthy volunteers than in patients with suspected renal failure [52]. GFR has been quantitated in $n = 1$ study with ^{68}Ga-EDTA [53], while ^{11}C-PABA has been shown to be safe in humans and could be used for functional renal imaging [54]. In a study by Baldelomar et al. [55], a mouse model was used to map nephron mass as proof of concept in a donated human kidney *in* vivo with RadioCF [55]. Higher renal artery F–Na–F uptake has also been associated with higher cardiovascular risk and lower GFR [56].

Discussion

Our systematic review assessed the application of PET imaging in the evaluation of renal metabolism in metabolic disorders based on 30 studies. The following key finding emerged. First, the largest proportion of studies reporting on kidney metabolism with PET were prospective reports. Second, ^{15}O-labeled water and ^{18}F-fluorodeoxyglucose were the most commonly used radiotracers for kidney metabolism. Third, a range of clinical features such as renal inflammation, glomerular filtration rate, and renal pathologies such as acute and chronic kidney diseases were studied with PET. Our findings reinforced the fact that PET imaging holds the potential for the assessment of renal function, and for the diagnosis of renal pathologies.

Renal physiology

Many tracers are cleared through the kidneys, which is why uptake appears high. This is the case with the widely used tracer ^{18}F-FDG. Several experimental tracers, most of which likely have no or very little true uptake in the kidneys, also show high renal uptake: ^{68}Ga-NODAGA-exendin-4 and ^{18}F-FP-(+)-DTBZ, used for β-cell imaging [57, 58], ^{18}F-Fluoro-L-DOPA, studied in infants with

congenital hyperinsulinism [59], ^{11}C-PK11195, used for assessing peripheral benzodiazepine receptor activity [60, 61], ^{18}F-AH111585, a peptide with a high affinity for the $\alpha_v\beta_3$ integrin receptor involved in angiogenesis [62], [1]C-PE2I, a cocaine analog tracer [63], ^{11}C-PIB and ^{18}F-FPYBF-2, which are amyloid imaging agents [64, 65], ^{11}C-nicotine, used to detect nicotine receptors [59], ^{11}C-metformin, used for studying the biodistribution and excretion of metformin [66], ^{11}C-MP4B, a tracer for the assessment of butyrylcholinesterase activity [67], [86]Y-SMT487, a radiolabeled somatostatin analogue [68] and ^{68}Ga-NOTA-UBI, a potential tracer for diagnosing infectious processes [69].

Renal perfusion

Clearance-based methods used to estimate effective renal plasma flow (ERPF) are time consuming and stressful to the patient [48]. PET provides a noninvasive method for the quantification of renal perfusion [70]. Alternatively, current modalities such as magnetic resonance imaging (MRI) arterial spin labelling (ASL) technique utilizes magnetic labelling and endogenous tracer of water in arterial blood to generate maps of absolute regional perfusion without the use of exogenous contrast [71].

[15]O-H$_2$O, also called "radiowater", is the most commonly used tracer for measuring renal perfusion [33]. Damkjær et al. showed that even medullar blood flow can be separately assessed with radiowater [34]. Several studies investigating physiological mechanisms have been conducted with radiowater. Modest saline loading, which leads to a natriuretic response, did not always induce changes in renal perfusion in seven healthy subjects [34]. When the ACE inhibitor quinaprilat was given as an injection to $n = 8$ patients with hypertension and moderate chronic heart failure, renal blood flow was increased [32]. Enalapril also increases renal perfusion [33]. Middlekauff et al. observed decreased renal perfusion due to vasoconstriction in $n = 29$ healthy subjects in response to a static handgrip exercise [30]. The magnitude and duration of this effect were exaggerated in $n = 39$ heart failure patients, compared to $n = 38$ controls [31]. Middlekauff et al. [29] also investigated pulmonary baroreflex in $n = 8$ heart failure patients and noted that reflex control of circulation in the forearm but not kidneys was abnormal compared to $n = 10$ controls [29]. Radiowater was used to measure regional hemodynamics and metabolism in obese subjects and non-obese controls to determine the effects of major weight loss before and after bariatric surgery [38]. Cortical perfusion was found to be significantly higher as compared with medullary perfusion in both groups. Even though cortical and medullary blood perfusion rates (ml/100 g/min) were not different between the two groups, total renal blood flow

was higher in the obese individuals, and it was significantly decreased following weight loss [38].

Three other PET tracers have also been shown to be usable in humans for the assessment of renal blood flow. Normand et al. validated a modeling method for [^{11}C] acetate to measure perfusion, using radiowater as gold standard [37]. The benefit of the tracer is that it can also be used to measure oxidative metabolism and can thus provide information on two different functions [37]. ^{13}N-ammonia has also been validated for measuring perfusion [28], but has since not been utilized in kidney studies. It is instead used in myocardial perfusion and blood flow studies [72]. [82]Rb is also most commonly used to assess myocardial blood flow in patients suspected of ischemic heart disease, but [82]Rb is also appropriate for modelling renal blood flow using dynamic PET methods, since the method has shown high image quality [41]. In a study assessing myocardial perfusion, regadenoson was shown to also increase kidney perfusion [42]. Another potential tracer for evaluating renal perfusion would be [62]Cu-ETS [35], but so far validation results in humans comparing the tracer with radiowater, have only been presented as a meeting report [40].

Renal metabolism

Renal substrate metabolism is closely tied to renal hemodynamics; the well-perfused renal cortex is rich in mitochondria and depends predominantly on oxidative metabolism—mainly of fatty acids, but also of ketone bodies, and lactate, whereas the renal medulla, which operates in relative hypoxia, relies predominantly on glycolysis [73]. The proximal tubules are also equipped with the enzymes responsible for gluconeogenesis (glucose 6-phosphatase, fructose 1,6 diphosphatase, and phosphoenolpyruvate carboxykinase), making the kidney one of the organs which contribute to endogenous glucose production after the liver, and also to a lesser extent the intestines [74].

PET provides a method for investigating kidney energy metabolism in humans in vivo, yet very few studies have addressed these questions so far. ^{11}C-acetate can be used for direct estimates of renal oxygen consumption [37]. It has recently been shown that renal FFA (i.e., cortical, and medullary) uptake using FTHA is increased in morbidly obese subjects compared to lean individuals, and that 6 months following bariatric surgery, renal FFA uptake remains high, because of the ongoing catabolic state [38]. ^{18}F-FDG is a widely available tracer, which can be used for studying metabolic shifts in glucose utilization [75]. To the best of our knowledge thus far, there has been no study evaluating renal glucose uptake using [18]FDG-PET. [18]FDG is excreted into urine and thus addressing renal metabolism with ^{18}F-FDG with current modeling methods is considered thus far to be heavily biased [76]. If the challenges with modeling

kidney tracer uptake could be overcome, ^{18}F-FDG could be used for studying metabolic shifts in kidneys as well. Since kidney energy metabolism is suggested to take part in the development of pathologies such as renal hypertension [74], PET has unused potential in investigating the development of these diseases in humans.

Renal function

Glomerular filtration rate (GFR) is defined as the rate of plasma flow through the glomerulus into the urinary space of the Bowman's capsule and is the most effective index and key indicator for renal function [77]. GFR is of high clinical significance especially in the detection, treatment, and prevention of kidney disease, but it cannot discern between one- or two-sided defects in filtration rate.

The most commonly used PET radio tracer for examinations of renal functions is [18]FDG. Pharmacokinetically, [18]FDG enters the kidney through renal arteries, is filtered in the glomeruli, then partially reabsorbed in the proximal tubule, and finally excreted in the urine [78, 79]. As partly mentioned in the results, early [18]FDG clearance (from injection) may also be used to estimate glomerular filtration rate (GFR) [48]. Both the cortex and total kidney [18]FDG glomerular filtration rate [$GFR_{(FDG)}$] were shown to have strong positive correlations with the reference value for GFR [$GFR_{(ref)}$] [48]. The $GFR_{(FDG)}$ was obtained from a regression analysis of Patlak plots [48], whereas the $GFR_{(ref)}$ was estimated from creatinine values using the Chronic Kidney Disease Epidemiology Collaboration (CKD-EPI) equation [80]. Based on this, it was estimated that GFR and EPRF can be assessed with [18]FDG-PET in healthy kidneys [48]. FDG renal clearance has since been utilized to also estimate urinary glucose loss [81]. Rasul et al. have shown that mean transit time of [18]FDG decreased with 2 weeks of SGLT2i treatment in T2D patients, shifting the transit time towards that of healthy controls [50].

Renal failure is characterized by the significant loss of kidney function with a GFR of less than 15 ml/min/1.73m^2 [82]. Available treatment options for end-stage renal failure include kidney transplantation, hemodialysis, and peritoneal dialysis [83]. Although [18]FDG-PET/CT can differentiate kidneys with end-stage renal disease from healthy kidneys, this by itself would be of limited clinical utility for patients who are already dependent on renal replacement therapy. Research shows that in patients with normal functioning kidneys, roughly 10% of the injected [18]FDG is excreted in the urine in about 70 min after the tracer injection [84]. However, in individuals with chronic kidney failure (CKF) who are on hemodialysis, urinary [18]FDG excretion is impaired and hence these subjects experience constant volume overload [85]. The [18]FDG tracer is distributed more in regions such as brain, and less in the cardiovascular system compared to control subjects without CKD [52].

Assessment of GFR can also be done using ^{68}Ga-EDTA [53] and [68]Ga [15]. This agrees with Hofman et al. [86] who reported that ^{68}Ga-GFR agreed well with ^{51}Cr-GFR for estimation of GFR. It was also stated that PET dynamic imaging offers a method to estimate GFR with an added advantage of enabling renal imaging in a single study [86]. There was good agreement between ^{68}Ga and [51]Cr- EDTA GFR despite injection of both radiotracers simultaneously and the use of the same samples for positron and gamma counting [86]. Hofman et al. [86] showed that [51]Cr- EDTA overestimates a GFR by about 10%. Despite this occurrence, Goethals et al. [87] stated that ^{51}Cr-EDTA is accepted as the most reliable agent to study whole kidney GFR. The ability of PET to quantify activity in three dimensions makes it ideal for applications such as GFR estimation [86].

Renal vasculature

Renal artery stenosis is a form of atherosclerotic vascular disease and can result in kidney insufficiency and renal hypertension [36]. Few studies have addressed effects of renal vasculature with PET in humans. Higher renal artery wall F-NaF activity was associated with CV risk and inversely associated with GFR in a group with high CV risk [56]. In an observational study by Koivuviita et al. [36], it was shown that angiographic severity of renal artery stenosis did not determine the perfusion response to revascularization. They hypothesized that it might be due to concomitant microvascular disease [36].

PET as a diagnostic tool

We have previously discussed the impact of tracer secretion in renal insufficiency and have identified how FDG secretion is impaired. This could be of concern, since FDG is a commonly used tracer in oncology and in the diagnostic work up of fever of unknown origin, and renal failure is very common in a clinical setting. Although compromised kidneys tend to alter the biodistribution of drugs cleared by the renal systems, the presentation of renal diseases do not necessarily impact FDG uptake values in other organs and, therefore, tracer dose adjustment is not required in such subjects [83].

Two studies have assessed [18]FDG PET/CT in the diagnostic work up of fever of unknown origin in end-stage renal disease patients, treated with dialysis. In a retrospective study on $n = 22$ patients, 15 patients showed metabolically active lesions and the scans lead to a change in treatment in 21 patients [88]. In a retrospective study on $n = 46$, 22 out of 46 scans identified the cause and a higher C-reactive protein level was predictive of a positive outcome [89]. The clinical utility was comparable to unselected patient populations. In

a case study, including seven PET scans on three patients with autosomal dominant polycystic kidney disease, [18]FDG PET could be used to diagnose or rule out cyst infection [90]. High [18]FDG uptake can also be caused by urinary calculi [91].

Slowly progressing chronic kidney disease is common in kidney transplants, but PET has not been widely utilized for assessing this pathology. A pilot study showed that PET could measure kidney transplant perfusion and that microvascular dysfunction could be detected in transplants [39]. Larger studies are needed on transplant patients and patients with advanced CKD before the method can be implemented in clinical use.

Acute kidney injury caused by acute rejection (AR) is also common in renal transplants. Current immunosuppressive treatments can efficiently treat AR, and thus the timely diagnosis of AR is fundamental. In acute rejection, there is accumulation of activated leucocytes in the transplant, which are characterized by an increased avidity for glucose (and [18]FDG) [92]. Diagnosis of AR is based on transplant needle biopsy, which is an invasive procedure. PET could, therefore, provide a noninvasive means for directing further diagnostic testing.

In a preclinical study in rats, Reuter and colleagues demonstrated, that [18]FDG-PET uptake was increased in transplants which were undergoing AR [93]. This finding was later confirmed in a study in $n = 31$ humans [45]. However, in this study, even though the sensitivity of [18]FDG-PET was 100%, the specificity was only 50% [45]. Jadoul et al. [44] later showed in a prospective $n = 95$ study that [18]FDG is usable for disproving acute rejection since quantification was repeatable and reproducible [44]. Parameters obtained from [18]FDG PET/MRI have also shown a possible predictive feature for renal recovery in solid organ kidney transplantation patients undergoing acute kidney injury [51]. ^{68}Ga-pentixafor has been investigated in 13 patients with renal allografts and complicated urinary tract infection, to detect leukocytes in grafts [47].

A cross-sectional diagnostic test study by Aaltonen et al. [94], where 26 dialysis patients suspected for renal osteodystrophy were studied with ^{18}F-NaF, showed that PET could provide a noninvasive diagnostic tool in patients that usually undergo bone biopsy for diagnosis [94].

Strengths and limitations

This review has followed the recommendations for the systematic search of articles and the PRSIMA statement, which is internationally recognized. The limitation of this study is that only single studies have been conducted for several PET tracers, such as ^{11}C-acetate, [18]FFTHA, ^{18}F-NaF, RadioCF, ^{11}C-PABA, ^{13}N-ammonia ^{18}F-FDS, ^{68}Ga-pentixafor and ^{68}Ga-EDTA, which importantly reduced the analytical

and comparative possibilities of our report. Nevertheless, we have maintained the descriptive axis of a systematic review to inform about this publication pitfalls and current knowledge gaps.

Conclusion

PET imaging provides an effective modality for evaluating a range of metabolic functions including glucose and fatty acid uptake, oxygen consumption and renal perfusion. Patients may benefit from undergoing PET imaging of the renal system for a variety of purposes, including the assessment of renal function and metabolism, disease diagnosis and prognosis. However, several useful tracers, however, have only been marginally utilized in clinical studies. PET imaging is an effectively growing, and currently underused modality for the noninvasive evaluation of renal (patho) physiology and its expansion could benefit non-oncological patients who suffer from metabolic diseases.

Declarations

References

1. Ogobuiro I, Tuma F. Physiology, renal. In: StatPearls. Treasure Island: StatPearls Publishing LLC; 2021. NBK538339 [bookaccession]

2. Gerich JE, Meyer C, Woerle HJ, Stumvoll M (2001) Renal gluconeogenesis: Its importance in human glucose homeostasis. Diabetes Care 24(2):382–391

3. Gerich JE (2010) Role of the kidney in normal glucose homeostasis and in the hyperglycaemia of diabetes mellitus: therapeutic implications. Diabetic Med 27:136–142

4. Joven J, Vilella E (1993) Lipoprotein heterogeneity in end-stage renal disease. Kidney Int 43:410–418

5. Webster AC, Bardhan M (2017) Chronic kidney disease. Lancet 389(10075):1238–1252

6. Guder WG, Wagner S, Wirthensohn G (1986) Metabolic fuels along the nephron: pathways and intracellular mechanisms of interaction. Kidney Int 29:41–45

7. Hems R, Ross B (1980) The metabolic fate of lactate in renal cortical tubules. Biochem J 190:27–37

8. Song P, Onishi A, Koepsell H, Vallon V (2016) Sodium glucose cotransporter SGLT1 as a therapeutic target in diabetes mellitus. Expert Opin Ther Targets 20(9):1109–1125

9. Blaine J, Chonchol M, Levi M (2015) Renal control of calcium, phosphate, and magnesium homeostasis. Clin J Am Soc Nephrol 10(7):1257–1272

10. Guertl B, Noehammer C, Hoefler G (2000) Metabolic cardiomyopathies. Int J Exp Pathol 81(6):349–372

11. Wang Y, Chen X, Song Y, Caballero B, Cheskin LJ (2008) Association between obesity and kidney disease: a systematic review and meta-analysis. Kidney Int 73(1):19–33

12. Klahr S, Levey AS, Beck GJ et al (1994) The effects of dietary protein restriction and blood-pressure control on the progression of chronic renal disease. Modification of diet in renal disease study group. N Engl J Med 330(13):877–884

13. Diabetes Control and Complications Trial Research Group, Nathan DM, Genuth S et al (1993) The effect of intensive treatment of diabetes on the development and progression of long-term complications in insulin-dependent diabetes mellitus. N Engl J Med 329(14):977–986

14. Slee AD (2012) Exploring metabolic dysfunction in chronic kidney disease. Nutr Metab (Lond) 9(1):1–16

15. Werner R, Xinyu C (2019) The next era of renal radionuclide imaging: Novel PET radiotracers. Eur J Nucl Med Mol Imaging 46(9):1773–1786

16. Juillard L, Janier MF, Fouque D et al (2000) Renal blood flow measurement by positron emission tomography using 15O-labeled water. Kidney Int 57(6):2511–2518

17. Patlak CS, Blasberg RG (1985) Graphical evaluation of blood-to-brain transfer constants from multiple-time uptake data generalizations. J Cereb Blood Flow Metab 5(4):584–590

18. Rebelos E, Immonen H, Bucci M et al (2019) Brain glucose uptake is associated with endogenous glucose production in obese patients before and after bariatric surgery and predicts metabolic outcome at follow-up. Diabetes Obes Metab 21(2):218–226

19. Oldgren J, Laurila S, Åkerblom A et al (2021) Effects of 6 weeks of treatment with dapagliflozin, a sodium-glucose co-transporter-2 inhibitor, on myocardial function and metabolism in patients with type 2 diabetes: A randomized, placebo-controlled, exploratory study. Diabetes Obes Metab 23:1505–1517

20. Immonen H, Hannukainen JC, Iozzo P et al (2014) Effect of bariatric surgery on liver glucose metabolism in morbidly obese diabetic and non-diabetic patients. J Hepatol 60(2):377–383

21. Ng JM, Bertoldo A, Minhas DS et al (2014) Dynamic PET imaging reveals heterogeneity of skeletal muscle insulin resistance. J Clin Endocrinol Metab 99(1):E102–E106

22. Dadson P, Landini L, Helmio M et al (2016) Effect of bariatric surgery on adipose tissue glucose metabolism in different depots in patients with or without type 2 diabetes. Diabetes Care 39(2):292–299

23. Dadson P, Ferrannini E, Landini L et al (2017) Fatty acid uptake and blood flow in adipose tissue compartments of morbidly obese subjects with or without type 2 diabetes: effects of bariatric surgery. Am J Physiol Endocrinol Metab 313(2):E175–E182

24. Moher D, Shamseer L, Clarke M et al (2015) Preferred reporting items for systematic review and meta-analysis protocols (PRISMA-P) 2015 statement. Syst Rev 4(1):1–9

25. Institute JB (2020) Critical appraisal tools for use in JBI systematic reviews checklist for prevalence studies. The University of Adelaide, Adelaide

26. Barrios L, Bergstrom K (2016) Radiolabeled sugars used for PET and SPECT imaging. Curr Radiopharm 9:180–186

27. Inaba T, Yamashita M, Kawase Y, Nakahashi H, Watanabe H (1989) Quantitative measurement of renal plasma flow by positron emission tomography with oxygen-15 water. Tohoku J Exp Med 159(4):283–289

28. Nitzschem EU, Choi Y, Killion D, Hoh CK, Hawkins RA, Schelbert R (1993) Quantification and parametric imaging of renal cortical blood flow in vivo based on patlak graphical analysis. Kidney Int 44(5):985–996

29. Middlekauff HR, Nitzsche EU, Hamilton MA et al (1995) Evidence for preserved cardiopulmonary baroreflex control of renal cortical blood flow in humans with advanced heart failure: a positron emission tomography study. Circulation 92:395–401

30. Middlekauff HR, Nitzsche EU, Nguyen AH, Hoh CK, Gibbs GG (1997) Modulation of renal cortical blood flow during static exercise in humans. Circ Res 80(1):62–68

31. Middlekauff HR, Nitzsche EU, Hoh CK et al (2000) Exaggerated renal vasoconstriction during exercise in heart failure patients. Circulation 101(7):784–789

32. Juillard L, Janier MF, Fouque D et al (2002) Dynamic renal blood flow measurement by positron emission tomography in patients with CRF. Am J Kidney Dis 40(5):947–954. https://doi.org/10.1053/ajkd.2002.36325

33. Kudomi N, Koivuviita N, Liukko KE et al (2009) Parametric renal blood flow imaging using [15O]H2O and PET. Eur J Nucl Med Mol Imaging 36(4):683–691

34. Damkjær M, Vafaee M, Braad PE, Petersen H, Høilund-Carlsen PF, Bie P (2012) Renal cortical and medullary blood flow during modest saline loading in humans. Acta physiol 205(4):472–483

35. Green MA, Hutchins GD (2011) Positron emission tomography (PET) assessment of renal perfusion. Semin Nephrol 31(3):291–299

36. Koivuviita N, Liukko K, Kudomim N et al (2012) The effect of revascularization of renal artery stenosis on renal perfusion in patients with atherosclerotic renovascular disease. Nephrol Dialysis Transp 27(10):3843–3848

37. Normand G, Lemoine S, Le Bars D et al (2019) PET [(11)C] acetate is also a perfusion tracer for kidney evaluation purposes. Nucl Med Biol 76–77:10–14

38. Rebelos E, Dadson P, Oikonen V et al (2019) Renal hemodynamics and fatty acid uptake: effects of obesity and weight loss. Am J Physiol Endocrinol Metab 317(5):E871–E878

39. Päivärinta J, Oikonen V, Räisänen-Sokolowski A et al (2019) Renal vascular resistance is increased in patients with kidney transplant. BMC Nephrol 20(1):437

40. Lacy J, Guerrero L, Christian B, Stone C (2010) Renal perfusion with ^{62}cu-ETS in comparison with ^{15}O-water PET. J Nucl Med 51(supplement 2):587–587

41. Tahari AK, Bravo PE, Rahmim A, Bengel FM (2014) Initial human experience with rubidium-82 renal PET/CT imaging. J Med Imaging Radiat Oncol 58:25–31

42. Keramida G, Gregg S, Peters AM (2020) Stimulation of the hepatic arterial buffer response using exogenous adenosine: hepatic rest/stress perfusion imaging. Eur Radiol 30(11):5852–5861

43. Guglielmo P, Ekström S, Strand R et al (2020) Validation of automated whole-body analysis of metabolic and morphological parameters from an integrated FDG-PET/MRI acquisition. Sci Rep 10(1):5331

44. Jadoul A, Lovinfosse P, Bouquegneau A et al (2020) Observer variability in the assessment of renal F-FDG uptake in kidney transplant recipients. Sci Rep 10(1):4617

45. Lovinfosse P, Weekers L, Bonvoisin C et al (2016) Fluorodeoxyglucose F(18) positron emission tomography coupled with computed tomography in suspected acute renal allograft rejection. Am J Transplant 16(1):310–316

46. Werner RA, Ordonez AA, Sanchez-Bautista J et al (2019) Novel functional renal PET imaging with 18F-FDS in human subjects. Clin Nucl Med 44(5):410–411

47. Derlin T, Gueler F, Bräsen JH et al (2017) Integrating MRI and chemokine receptor CXCR4-targeted PET for detection of leukocyte infiltration in complicated urinary tract infections after kidney transplantation. J Nucl Med 58(11):1831–1837

48. Geist B, Baltzer P, Fueger B, Hamboeck M, Hacker M, Staudenherz A (2018) Assessing the kidney function parameters glomerular filtration rate and effective renal plasma flow dynamic FDG-PET/MRI in healthy subjects. EJNMMI Res 8:37

49. Qiao H, Bai J, Chen Y, Tian J (2008) Modeling the excretion of FDG in human kidneys using dynamic PET. Comput Biol Med 38(11):1171–1176. https://doi.org/10.1016/j.compbiomed.2008.09.006

50. Rasul S, Geist BK, Brath H et al (2020) Response evaluation of SGLT2 inhibitor therapy in patients with type 2 diabetes mellitus using 18F-FDG PET/MRI. BMJ Open Diabetes Res Care 8(1):e001135

51. Pajenda S, Rasul S, Hacker M, Wagner L, Geist BK (2020) Dynamic 2-deoxy-2[18F] fluoro-D-glucose PET/MRI in human renal allotransplant patients undergoing acute kidney injury. Sci Rep 10(1):8270

52. Minamimoto R, Takahashi N, Inoue T (2007) FDG-PET of patients with suspected renal failure: Standardized uptake values in normal tissues. Ann Nucl Med 21(4):217–222

53. Yamashita M, Inaba T, Kawase Y et al (1988) Quantitative measurement of renal function using ga-68-EDTA. Tohoku J Exp Med 155(2):207–208

54. Ruiz-Bedoya CA, Ordonez AA, Werner RA et al (2020) C-PABA as a PET radiotracer for functional renal imaging: preclinical and first-in-human study. J Nucl Med 61(11):1665–1671

55. Baldelomar EJ, Reichert DE, Shoghi KI et al (2021) Mapping nephron mass in vivo using positron emission tomography. Am J Physiol Renal Physiol 320(2):F183–F192 (**Epub 2020 Dec 7**)

56. Oliveira-Santos M, McMahon G, Castelo-Branco M et al (2020) Renal artery wall 18F-NaF activity and glomerular filtration rate: an exploratory analysis in a high cardiovascular risk population. Nucl Med Commun 41(2):126–132

57. Boss M, Buitinga M, Jansen TJP, Brom M, Visser EP, Gotthardt M (2020) PET-based human dosimetry of ^{68}ga-NODAGA-exendin-4, a tracer for β-cell imaging. J Nucl Med 61(1):112–116

58. Naganawa M, Lim K, Nabulsi NB et al (2018) Evaluation of pancreatic VMAT2 binding with active and inactive enantiomers of FFP-DTBZ in healthy subjects and patients with type 1 diabetes. Mol Imaging Biol 20(5):835–845

59. Garg PK, Lokitz SJ, Truong L et al (2017) Pancreatic uptake and radiation dosimetry of 6-[18F]fluoro-L-DOPA from PET imaging studies in infants with congenital hyperinsulinism. PLoS ONE 12(11):e0186340

60. Roivainen A, Någren K, Hirvonen J et al (2009) Whole-body distribution and metabolism of [N-methyl-11C](R)-1-(2-chlorophenyl)-N-(1methylpropyl)-3-isoquinolinecarboxamide in humans; an imaging agent for in vivo assessment of peripheral benzodiazepine receptor activity with positron emission tomography. Eur J Nucl Med Mol Imaging 36(4):671–682

61. Kumar A, Muzik O, Chugani D, Chakraborty P, Chugani HT (2009) PET-derived biodistribution and dosimetry of the benzodiazepine receptor-binding radioligand (11C)-(R)-PK11195 in children and adults. J Nucl Med 51(1):139–144

62. McParland BJ, Miller MP, Spinks TJ, Kenny LM, Osman S, Cohen PS (2008) The biodistribution and radiation dosimetry of the arg-gly-asp peptide 18F-AH111585 in healthy volunteers. J Nucl Med 49(10):1664–1667

63. Ribeiro MJ, Ricard M, Lièvre MA, Bourgeois S, Emond P, Syrota A (2007) Whole-body distribution and radiation dosimetry of the dopamine transporter radioligand [(11)C]PE2I in healthy volunteers. Nucl Med Biol 34(4):465–470

64. Scheinin NM, Tolvanen TK, Wilson IA, Arponen EM, Någren KA, Rinne JO (2007) Biodistribution and radiation dosimetry of the amyloid imaging agent 11C-PIB in humans. J Nucl Med 48(1):128–133

65. Nishii R, Higashi T, Kagawa S, Okuyama C, Saji H, Yamauchi H (2018) 18F-FPYBF-2, a new F-18 labelled amyloid imaging PET tracer: biodistribution and radiation dosimetry assessment of first-in-man 18F-FPYBF-2 PET imaging. Ann Nucl Med 32(4):256–263

66. Gormsen LC, Sundelin EI, Jensen JB et al (2016) In vivo imaging of human 11C-metformin in peripheral organs: dosimetry, biodistribution, and kinetic analyses. J Nucl Med 57(12):1920–1926

67. Roivainen A, Rinne J, Virta J et al (2004) Biodistribution and blood metabolism of 1–11C-methyl-4-piperidinyl n-butyrate inhumans: an imaging agent for in vivo assessment of butyrylcholinesterase activity with PET. J Nucl Med 45(12):2032–2039

68. Jamar F, Barone R, Mathieu I et al (2003) 86Y-DOTA0)-D-Phe1-Tyr3-octreotide (SMT487)—a phase 1 clinical study: Pharmacokinetics, biodistribution and renal protective effect of different regimens of amino acid co-infusion. Eur J Nucl Med Mol Imaging 30(4):510–518

69. Ebenhan T, Sathekge MM, Lengana T et al (2018) Ga-NOTA-functionalized ubiquicidin: cytotoxicity, biodistribution, radiation dosimetry, and first-in human PET/CT imaging of infections. J Nucl Med 59(2):334–339

70. Champion C, Loirec C (2007) Positron follow-up in liquid water: II. Spatial and energetic study for the most important radioisotope used in PET. Phys Med Biol 52:6605–6625

71. Odudu A, Nery F, Harteveld AA et al (2018) Arterial spin labelling MRI to measure renal perfusion: a systematic review and statement paper. Nephrol Dial Transplant 33(suppl_2):ii15–ii21

72. Iskandrian AE, Dilsizian V, Garcia EV et al (2018) Myocardial perfusion imaging: lessons learned and work to be done-update. J Nucl Cardiol 25(1):39–52

73. Meury L, Noël J, Tejedor A, Sénécal J, Gougoux A, Vinay P (1994) Glucose metabolism in dog inner medullary collecting ducts. Ren Physiol Biochem 17(5):246–266

74. Tian Z, Liang M (2021) Renal metabolism and hypertension. Nat Commun 12(1):1–12

75. Nuutila P, Koivisto VA, Knuuti J et al (1992) Glucose-free fatty acid cycle operates in human heart and skeletal muscle in vivo. J Clin Invest 89(6):1767–1774

76. Qiao H, Bai J, Chen Y, Tian J (2008) Modeling the excretion of FDG in human kidneys using dynamic PET. Comput Biol Med 38(11–12):1171–1176

77. Kaufman DP, Basit H, Knohl SJ. Physiology, glomerular filtration rate. In: StatPearls. Treasure Island: StatPearls Publishing LLC; 2021. NBK500032 [bookaccession].

78. Landau BR, Spring-Robinson CL, Muzic RF Jr et al (2007) 6-fluoro-6-deoxy-D-glucose as a tracer of glucose transport. Am J Physiol Endocrinol Metab 293(1):E237–E245

79. Scafoglio C, Hirayama BA, Kepe V et al (2015) Functional expression of sodium-glucose transporters in cancer. Proc Natl Acad Sci U S A 112(30):E4111–E4119

80. Levey AS, Stevens LA, Schmid CH et al (2009) A new equation to estimate glomerular filtration rate. Ann Intern Med 150(9):604–612

81. Latva-Rasku A, Honka MJ, Kullberg J et al (2019) The SGLT2 inhibitor dapagliflozin reduces liver fat but does not affect tissue insulin sensitivity: a randomized, double-blind, placebo-controlled study with 8-week treatment in type 2 diabetes patients. Diabetes Care 42(5):931–937

82. Phoon RK (2012) Chronic kidney disease in the elderly—assessment and management. Aust Fam Physician 41(12):940–944

83. Kode V, Karsch H, Osman MM, Muzaffar R (2017) Impact of renal failure on F18-FDG PET/CT scans. Front Oncol 7:155

84. Bach-Gansmo T, Dybvik J, Adamsen T, Naum A (2012) Variation in urinary excretion of FDG, yet another uncertainty in quantitative PET. Acta Radiol Short Rep 1(8):1–3. https://doi.org/10.1258/arsr.2012.120038 (**eCollection 2012**)

85. Toriihara A, Kitazume Y, Nishida H, Kubota K, Nakadate M, Tateishi U (2015) Comparison of FDG-PET/CT images between chronic renal failure patients on hemodialysis and controls. Am J Nucl Med Mol Imaging 5(2):204–211

86. Hofman M, Binns D, Johnston V et al (2015) 68Ga-EDTA PET/CT imaging and plasma clearance for glomerular filtration rate quantification: comparison to conventional 51Cr-EDTA. J Nucl Med 56(3):405–409

87. Goethals P, Volkaert A, Vandewielle C, Dierckx R, Lameire N (2000) 55Co-EDTA for renal imaging using positron emission tomography (PET): a feasibility study. Nucl Med Biol 27(1):77–81

88. Tek CK, Chennu KK, Amancharla YL, Manthri GR, Rapur R, Vishnubotla SK (2017) Utility of 18 F-FDG PET/CT scan to diagnose the etiology of fever of unknown origin in patients on dialysis. Hemodial Int 21(2):224–231

89. Lawal IO, Popoola GO, Lengana T, Ankrah AO, Ebenhan T, Sathekge M (2019) Diagnostic utility of F-FDG PET/CT in fever of unknown origin among patients with end-stage renal disease treated with renal replacement therapy. Hellenic J Nucl Med 22(1):70–75

90. Bleeker-Rovers CP, de Sévaux RG, van Hamersvelt HW, Corstens FH, Oyen WJ (2003) Diagnosis of renal and hepatic cyst infections by 18-F-fluorodeoxyglucose positron emission tomography in autosomal dominant polycystic kidney disease. Am J Kidney Dis 41(6):E18-21

91. Fu Z, Li Z, Huang J et al (2016) High (18)F-FDG uptake in urinary calculi on PET/CT: An unrecognized non-malignant accumulation. Eur J Radiol 85(8):1395–1399

92. Hanssen O, Erpicum P, Lovinfosse P et al (2017) Non-invasive approaches in the diagnosis of acute rejection in kidney transplant recipients. Part I. in vivo imaging methods. Clin Kidney J 10(1):97–105

93. Reuter S, Schnockel U, Schroter R et al (2009) Non-invasive imaging of acute renal allograft rejection in rats using small animal F-FDG-PET. PLoS ONE 4:e5296

94. Aaltonen L, Koivuviita N, Seppänen M et al (2020) Correlation between (18)F-sodium fluoride positron emission tomography and bone histomorphometry in dialysis patients. Bone 134:11526